Journal of Inorganic Biochemistry 199 (2019) 110782

Contents lists available at ScienceDirect

Journal of Inorganic Biochemistry

journal homepage: www.elsevier.com/locate/jinorgbio

Formation of gallic acid layer on γ-AlOOH nanoparticles surface and their antioxidant and membrane-protective activity

I.S. Martakov[a,*], O.G. Shevchenko[b], M.A. Torlopov[a], E.Yu. Gerasimov[c], P.A. Sitnikov[a]

[a] Institute of Chemistry of Komi Scientific Centre of the Ural Branch of the Russian Academy of Sciences, 167000, Syktyvkar, 48 Pervomayskaya St., Russian Federation
[b] Institute of Biology of Komi Scientific Centre of the Ural Branch of the Russian Academy of Sciences, 167982 Syktyvkar, 28 Kommunisticheskaya St., Russian Federation
[c] Boreskov Institute of Catalysis SB RAS, 5 Lavrentieva Av., 630090 Novosibirsk, Russian Federation

ARTICLE INFO

Keywords:
Alumina
Sol-gel method
Cytotoxicity
Antioxidant properties
Gallic acid
Membrane-protective activity
Oxidative hemolysis

ABSTRACT

In the reported study we prepared gallic acid modified γ-AlOOH nanoparticles. We proposed mechanism of phenolic compounds binding on the alumina, suggesting covalent and electrostatic interactions. Most of the properties of alumina nanoparticles (NPs) are unchanged, but there is partial reduction of surface charge. Prepared samples are colloidally stable hydrosols. It allowed us to perform biological studies on cellular and non-cellular models, which showed nontoxicity of both pure and hybrid γ-AlOOH nanoparticles. Furthermore, pure alumina NPs exhibit antioxidant properties, which are enhanced after gallic acid immobilization on their surface. Also, hybrid alumina-gallic acid NPs showed membrane-protective activity.

1. Introduction

Nanomedicine is a developing area in nanotechnology [1–4]. Nanoparticles (NPs) can be used ass delivery vehicles (drugs, enzymes, etc.) [5,6], contrast agents [7,8], for treatment of various diseases [9,10]. Despite the growing popularity and enormous prospects of this direction, there are potential dangers of using NPs in relation to living systems. The presence of NPs inside the body is able to initiate pathogenic processes—ion exchange disorder in cells, depolarization of the cell membrane [11], and, most likely, the formation of reactive oxygen species (ROS) [12–14]. The formation of ROS is associated with the presence of a developed NPs surface, high surface energy, the presence of hydroxyl groups in metal or silicon-oxide systems. It should be noted that the formation of ROS in itself is not a negative factor. Generation of ROS by NPs can be used for purification of water from organic pollutants [15,16] or even treating some diseases, e.g. cancer [17,18]. More dangerous is the imbalance of prooxidants-antioxidants in cells [19,20]. To prevent the formation of free radicals caused by NPs inactivation (e.g. PEGylation) of the surface is used [21,22] or, for example, immobilization of antioxidants on the surface of NPs. The use of compounds of plant origin for this purpose is promising from the standpoint of reducing toxicity and increasing biocompatibility. Phytomedicine offers a wide selection of natural antioxidants. One of the most well-known antioxidants are phenolic compounds, widely found in food and beverages [23,24]. For example, gallic acid (GA) is a part of tea tannins (gallates) [25]. This phenolic acid and its derivatives are widely used in the manufacture of cosmetics, food and pharmaceutical products. The biomedical potential of these compounds includes the use of highly relevant areas of neuroprotective [26,27] and safe antibacterial compounds with the effect of destruction of biofilms [28,29].

Gallic acid is used to coat silver nanoparticles, while simultaneously synthesizing them as a reducing agent and stabilizer [30,31]. The resulting nanoparticles are tested for their use in cancer therapy and as antimicrobial agents. The creation of a biocompatible coating - a gallic acid layer - on the surface of magnetite nanoparticles was studied in the work [32]. It is indicated that gallic acid under the conditions of the synthesis of such particles undergoes polymerization. Rashidi et al. [33] proposed SiO_2 particles coated with amine-containing compounds for transport and controlled release of GA. Unfortunately, in most studies where GA is used to form a biocompatible nanoparticle layer, there is no assessment of the cytotoxicity and antiradical activity of such a coating, its ability to inhibit the negative processes of peroxidation of cell membrane lipids.

One of the most convenient and widely used model objects in toxicology and pharmacology are mammalian red blood cells. These cells undergo serious changes not only when the complex of adverse factors is exposed to the organism, but also in vitro, which makes it useful for studying the mechanisms of toxicity and biological activity of various compounds, including heavy metals [34–38]. The erythrocyte is an extremely convenient cellular model for studying the development

* Corresponding author.
E-mail address: gmartakov@gmail.com (I.S. Martakov).

https://doi.org/10.1016/j.jinorgbio.2019.110782
Received 5 April 2019; Received in revised form 11 June 2019; Accepted 15 July 2019
Available online 16 July 2019

mechanisms of oxidative damage and the mechanisms of action of antioxidants [39–41]. In vitro experiments allow a correct assessment of the molecular cell aspects of the effects of various compounds and reduce the number of expensive animal studies.

To assess the antioxidant activity of various compounds, biological tissue homogenates containing proteins, DNA, RNA and lipids (cholesterol, galactolipids, individual phospholipids and gangliosides) can be used as a biological oxidation substrate as well (water-lipid emulsion) [42–49].

For research, we chose boehmite as one of the safest and approved by the FDA for use as an adjuvant [50,51]. However, there are a number of works in which the formation of ROS caused by aluminum compounds is detected [52]. Therefore, the purpose of this work was the creation of a biocompatible coating of NPs based on gallic acid and an assessment of its effectiveness—the ability to have antioxidant and membrane protective activity.

2. Materials and methods

2.1. Sol-gel synthesis of alumina sols and their modification with gallic acid

Alumina sol was prepared from aluminum isopropoxide by Yoldas method [53]. Briefly, Al(OPr-iso)$_3$ was added in a flask with preheated to 75 °C deionized water under vigorous stirring. After disappearance of large particles HCl was added to the flask. Molar composition of components was n(H2O):n(Al(OPr-iso)$_3$):n(HCl) = 200:1:0.07. Alumina was modified by adding calculated amount of gallic acid in a form of solution to the prepared sol. Prepared alumina and modified alumina sols were purified from loose low-molecular compounds by dialysis against water (cutoff = 2–4 kDa).

2.2. Samples characterization

X-ray diffraction (XRD) patterns of freeze-dried sols were recorded with the aid of an XRD-6000 Shimadzu diffractometer using CuK$_\alpha$ radiation (λ = 1.541 Å); anode voltage and current strength were equal to 30 kV and 30 mA, respectively. X-ray diffractograms were obtained over an angular range of 2θ = 10–80° with 0.1° increment. The structure and microstructure of powders were examined by high-resolution transmission electron microscopy (TEM) on a JEM-2010 electron microscope (JEOL, Japan) at an accelerating voltage of 200 kV and point-to-point resolution of 0.14 nm. Prior to electron-microscopic examination, the particles were immersed in ethanol and applied to holey carbon substrates (hole diameter ~1 μm) secured on copper grids. The particles were applied using ultrasonic processor (UZD-1UC2 (USSR), frequency - 12 kHz, type of sonification - tip), which allowed us to achieve a uniform distribution of the particles over the substrate surface. After the particles on the carbon substrate and grid were withdrawn from the ethanol, it was evaporated.

UV–vis spectra of liquid samples were recorded on Solar PB2201 spectrophotometer at 200–600 nm with 0.5 nm increment.

Hydrodynamic diameter of particles (*Z*-Average size) and zeta-potential values for 0.01 wt% aqueous solutions were measured by dynamic light scattering (DLS) and laser Doppler electrophoresis, respectively, using a Malvern Zetasizer Nano ZS instrument (4 mW He/Ne laser, 633 nm) at 25 °C in a DTS1070 disposable capillary cell (Malvern). All measurements were repeated at least three times. Isoelectric point was determined with background electrolyte 0.001 M KCl; pH value was changed by KOH dropwise addition.

Fourier-transform infrared (FTIR) spectra of freeze-dried samples were obtained using a Prestige 21 FTIR spectrometer ("Shimadzu", Japan). The measurements were carried out at 4 cm^{-1} intervals in the 400–4000 cm^{-1} region in diffuse reflection mode. Freeze-dried samples were mixed with crystalline KBr and placed into a diffuse reflection attachment; then, transmission spectra were obtained.

Acid-base surface properties were studied using an Aquilon ATP-02 automatic potentiometric titrator (Russia); pK spectra were obtained using the experimental titration curve of aqueous cellulose suspensions according to the technique proposed by Ryazanov & Dudkin (2009). All titrant solutions with 0.1 M concentration were prepared from standard solutions by volumetric dilution. The starting volume of titrated hydrosol was 50 ml, concentration was 6 mg/ml. Temperature of the titrated solution in thermostated cell was kept constant with 0.25 °C accuracy. The temperature of the titrated solution in the thermostated cell was 25 °C and kept constant with an accuracy of 0.25 °C. The solution was stirred with magnetic stirrer. The pH values were measured after addition of each titrant portion, and only after equilibrium was established (in 15–20 min). Titration was conducted in argon atmosphere in polypropylene vessels with constant concentrations of background electrolyte (KCl, 0.1, 0.01 and 0.001 M). Titrant injections of 0.1 ml and 0.03 ml were made near the potential jump. Every sample was titrated three times.

The content of gallic acid (phenolic acid, g/dispersed phase, g) in each AlOOH sol was determined with Folin-Ciocalteu reagent according to the method described in [55] with some changes: 200 μl of AlOOH-GA sol (1.0 mg/ml) was mixed with 200 μl of Folin-Ciocalteu reagent and 1500 μl of distilled water for 7 min, then 300 μl of sodium carbonate (Na_2CO_3, 20% wt.) was added. The mixture was shaken for 15 min at 50 ± 0.1 °C and then cooled in water. Absorbance at 765 nm was recorded using the spectrophotometer (Solar PB2201) relative to the original AlOOH sol with the same treatment. Calibration curve was obtained using gallic acid. Maximum content of GA was 2.0%. We investigated two types of hybrid particles – with low GA content (0.5%) and maximum content (2.0%); these samples are named AlOOH-GA-0.5 and AlOOH-GA-2.0 respectively. Control samples of gallic acid solutions are denoted as GA-0.5 and GA-2.0 for comparison with hybrid particles with the same concentration of GA.

2.3. Biological assays

2.3.1. Materials and methods

Experiments were conducted using the equipment of the Center of Collective Usage 'Molecular Biology', Institute of Biology, Komi Scientific Center, Ural Branch of RAS. Mice were obtained from the scientific collection of experimental animals at Institute of Biology, Komi Scientific Center, Ural Branch of RAS (http://www.ckp-rf.ru/usu/471933/) and were kept considering hygienic and bioethical aspects of working with laboratory animals in accordance with the corresponding regulations set by Institute of Biology. Absorption was measured using a Thermo Spectronic Genesys 20 instrument. Absorption spectra of hemolysates were analyzed on a Fluorat-02-Panorama spectrofluorimeter. Mice red blood cells (RBCs) were incubated in a thermostated Biosan ES-20 shaker. Each experiment was repeated 4–5 times. Statistical analysis was conducted using Microsoft Office Excel 2007 software packages. Reagent grade and pure grade phosphate-buffered saline (PBS, pH 7.4) (Sigma-Aldrich, USA), trichloroacetic acid (Sigma-Aldrich, Germany), thiobarbituric acid (Alfa Aesar, UK), ascorbic acid (ICN Biomedicals, USA) and $FeSO_4$ (Reachim Ltd., Moscow, Russian Federation) were used.

2.3.2. Antioxidant activity. TBARS assay

The antioxidant activity was evaluated in vitro as inhibition of accumulation of secondary lipid peroxidation products in mouse brain homogenates [42,47,49]. The brain was homogenized in physiological saline (pH 7.4) (10% v/v) and centrifuged at 3000 rpm for 10 min. The low-speed supernatant containing water, proteins, DNA, RNA, and lipids (cholesterol, galactolipids, individual phospholipids and gangliosides) was separated [42,43]. The test compounds were added to the supernatant in relation to 1:1, 1:3 and 1:9, then in 30 min lipid autoxidation was initiated by adding a freshly prepared $FeSO_4$ solution (3 μM) and ascorbic acid (300 μM) (Chawla, 2005; Kim, 2013). Samples were stirred gently during 1 h at 37 °C, then the reaction was stopped by

adding of trichloroacetic acid (20%) and of 2-thiobarbituric acid (0.7%). The reaction mixture was heated in a boiling water bath for 15 min. After cooling, the precipitate was removed by centrifugation (3000 rpm, 10 min). The concentration of secondary lipid peroxidation products reacting with 2-thiobarbituric acid (TBARS) was determined at λ 532 nm using the extinction coefficient of $1.56 \times 10^5\ M^{-1}\ cm^{-1}$ [49,56].

2.3.3. Mouse RBC test for toxicity, antioxidant and membrane-protective activity

The toxicity, antioxidant and membrane-protective activities were evaluated in 0.5% (v/v) suspension of mice RBCs in PBS. Toxicity was assessed by RBCs hemolysis after 1, 3 and 5 h of incubation with test compounds. Antioxidant and membrane-protective activities were determined by inhibition of H_2O_2-induced hemolysis, inhibition of lipid peroxidation products accumulation (TBARS assay), and oxidation of oxyhemoglobin in RBCs. After addition of the test compound solutions in relation to 1:9 and 1:49 the suspension of RBCs was incubated for 30 min, and then hemolysis was initiated by addition of H_2O_2 (final concentration 1.8 mM). The reaction mixture was shaken gently for 5 h at 37 °C. The aliquot was taken from incubation medium each hour and centrifuged for 5 min at 3000 rpm. Hemolysis was determined as hemoglobin content in the supernatant at λ 524 nm [41]. The percentage of hemolysis was calculated relative to complete hemolysis of the sample. The concentration of secondary lipid peroxidation products in RBC hemolysate was assayed using the formation of malondialdehyde as an indicator as described above. The reaction was stopped by adding trichloroacetic and 2-thiobarbituric acids. Samples were heating in a boiling water bath for 15 min, followed by centrifugation for 10 min at 1600*g* to remove the precipitated protein. The adduct of 2-thiobarbituric acid with malondialdehyde in the supernatant was measured by spectrophotometric method at λ 532 nm with the extinction coefficient of $1.56 \times 10^5\ M^{-1}\ cm^{-1}$ [49,56]. To assess the accumulation of hemoglobin oxidation products, the absorption spectrum of hemolysate was analyzed at λ values of 540–640 nm. The content of oxyhemoglobin (oxyHb) and methemoglobin (metHb) was calculated using corresponding extinction coefficients [57].

3. Results and discussion

3.1. Formation of pure and GA-modified NPs and their properties

The X-ray diffraction pattern of the obtained alumina indicates that the crystal structure of the sample is γ-AlOOH (pseudoboehmite) (Fig. 1) (JCPDS 00-049-0133) with broad peaks characteristic of nanocrystalline powders.

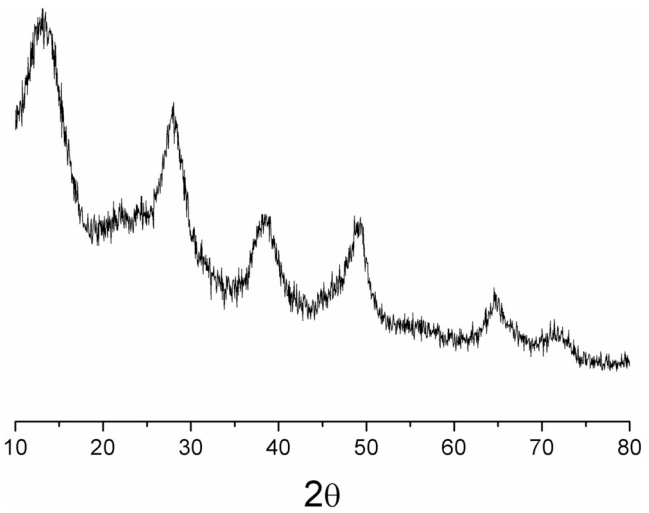

Fig. 1. XRD pattern of freeze-dried alumina sample.

The shape of the obtained nanoparticles is plate-like which is characteristic of layered boehmite [58], what follows from the TEM images (Fig. 2). Diameter of NPs is about 10–30 nm, thickness – 2–4 nm.

Alumina sol did not have peaks in the UV–Vis spectrum (Fig. 3). Non-zero absorption in the spectrum is associated with the scattering of light by nanoparticles. The GA spectrum has typical peaks at 215 nm and 264 nm, which are associated with vibrations of the benzene ring (Fig. 3). The hydroxyl and carboxyl groups of gallic acid are auxochromes. The peaks of gallic acid immobilized on the surface of the boehmite demonstrate a bathochromic shift (Fig. 3) (AlOOH-GA-2.0 sample). Shift can be caused by intensive interaction of GA with boehmite NPs.

Interaction of GA with boehmite led to a decrease in zeta-potential values (4) - from +49 it decreased to +34 mV. The maximum content of GA on boehmite was 2.0% according to the spectrophotometric determination with Folin-Ciocalteu reagent. If we consider our hybrid NPs for injection into the blood, reducing a positive charge can have a positive effect by reducing the intensity of interaction with blood components. The isoelectric point (IEP) of boehmite was 9.7 (Fig. 5). Since the particles are positively charged, they can electrostatically interact with GA. Hybrid NPs had almost the same value of the isoelectric point - 9.6 (Fig. 5). At pH ≤ 7.6, boehmite nanoparticles have a high positive charge and are resistant to aggregation. At higher pH values, zeta potential decreases sharply, and the NPs begin to coagulate; thus, the hydrodynamic size increases significantly (Fig. 5) and is about several micrometers. Micrometer aggregates tend to precipitate in the first minutes. If we consider a possible injection of AlOOH sols into the blood (for example, humans or mice) that have a pH of 7.35–7.45 [59,60], its colloidal stability in neutral and weakly basic solutions helps prevent homocoagulation of NPs. For a more detailed assessment of the surface properties of our compounds, we conducted potentiometric titration.

Based on the data of potentiometric titration of aqueous dispersions of boehmite, the acid-base properties of the surface of the initial compounds and boehmite nanoparticles coated with gallic acid were studied. The mathematical model used by us for the description of acidic and basic centers is pK spectroscopy [54] makes it possible to calculate, in the framework of the 2-pK model [61] surface complexation constants (pK_i) constants of the corresponding adsorption surface centers according to their ability, depending on the pH of the medium, to go into the acidic (pK_2) or basic (pK_1) forms, due to reactions with proton transfer, or to take into account the sorption of cations (pK_M) and anions (pK_A) of the background electrolyte. This approach also allows one to determine the concentration of the corresponding surface acid-base center of the compound with unknown chemical composition.

Titration of the surface of boehmite and AlOOH-GA sols was performed with 0.01 n KOH, therefore, the calculation of the values of surface complexation was carried out for the pK_M and pK_2 values.

In the case of gallic acid (Fig. 6a), $pK_a = 4.4 \pm 0.01$, the number of acid-base centers with this pK_a is $q_i = 5.89 \pm 0.04$ mmol/g. The obtained data, in terms of pK_a, are in good agreement with known literature data [62]

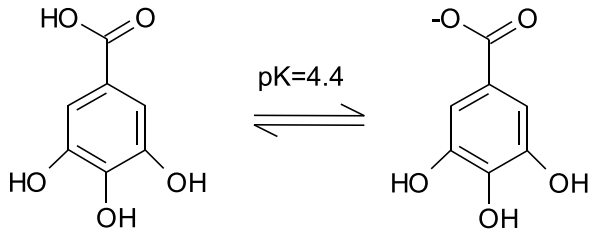

The pK spectrum of γ-AlOOH is shown in Fig. 7b. The spectrum contains the bands corresponding to the equilibria:

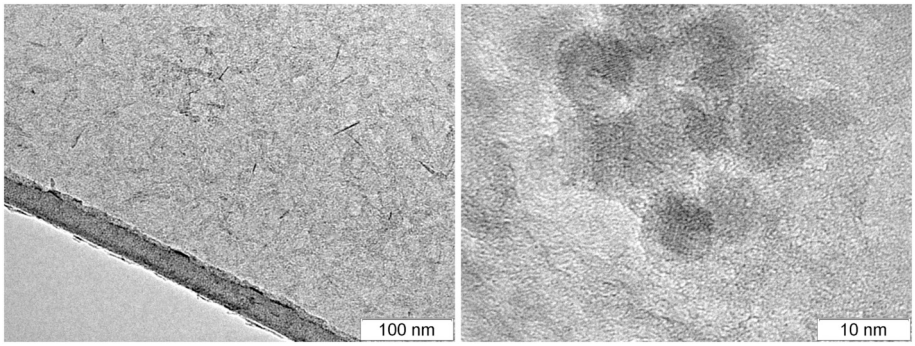

Fig. 2. TEM images of AlOOH nanoparticles.

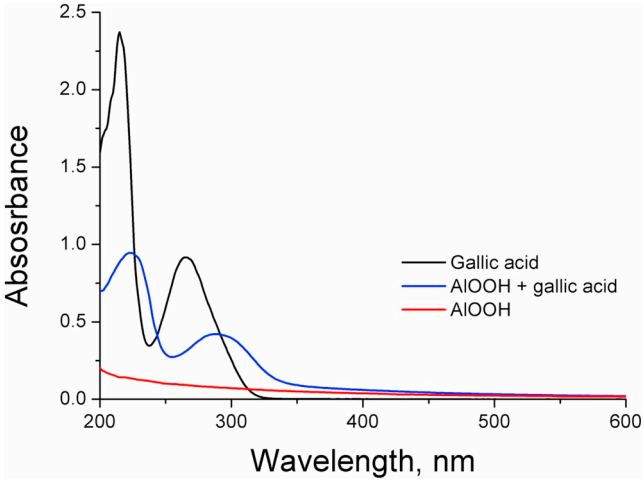

Fig. 3. UV–vis spectra of gallic acid, AlOOH sol and hybrid AlOOH-GA sol. (concentration of NPs – 0.6 mg/ml).

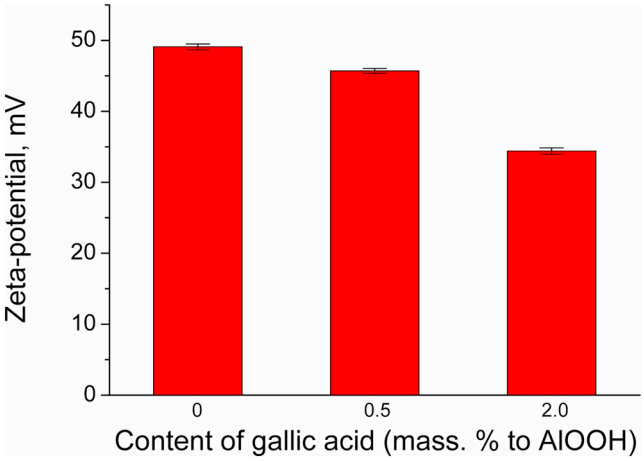

Fig. 4. Dependence of zeta potential on GA content on boehmite nanoparticles. (Vertical bars: mean ± SE) (concentration of NPs – 0.6 mg/ml).

$$-Al-OH + M^{+} \leftrightarrow -Al-O^{-}\cdots M^{+} + H^{+} \quad pK_{aM} = 7.10 \pm 0.05\ (q_M = 0.145\ mmol/g)$$

$$-Al-OH \leftrightarrow -Al-O^{-} + H^{+} \quad pK_{a2} = 8.70 \pm 0.03\ (q_2 = 0.316\ mmol/g)$$

The pK-spectrum of the hybrid particle contains the bands of both gallic acid $pK_a = 4.4$ ($q = 0.0399$ mmol/g) and aluminum oxyhydroxide $pK_M = 7.1$ ($q_M = 0.04$ mmol/g), $pK_2 = 8.6$ ($q_2 = 0.11$ mmol/g).

The introduction of gallic acid on the surface of alumina led to a decrease in the number of acid-base centers of boehmite involved in the formation of the electric double layer by about 3 times.

The amount of GA (0.0399 mmol/g or 2.8 wt%) bound to AlOOH NPs is a little higher than GA content, determined spectrophotometrically with Folin-Ciocalteu reagent (2.0%). The difference between the pK AlOOH and GA values is 8.6–4.4 = 4.2. The higher the ΔpK, the more intense the substances interact with each other, which means that acid-base interactions are more likely to participate besides van der Waals forces [63].

FTIR spectra of AlOOH show peaks associated with vibrations of Al – O bonds [64] (Fig. 7). The spectrum of GA has a peak at 1730 cm^{-1}, which corresponds to the vibrations of the carbonyl vibration (C = O) in carboxyl group. The spectrum of the AlOOH-GA sample has bands characteristic of boehmite and the most intensive ones for GA. The peak characteristic of the carboxyl group was shifted to 1600 cm^{-1} what could be assigned to asymmetric carboxylate stretch [65], which indicates its interaction with boehmite through covalent bonding and correlates well with similar systems described in literature [66]. Gallic acid can bind to boehmite via bridging and dentate bonds, as predicted in [67].

Thus, based on the results of potentiometric titration, FTIR spectroscopy and electrophoretic studies (particle size and charge), we can conclude that GA is immobilized on the AlOOH surface through two types of interactions—one part is only electrostatically bound, the other is chemically linked.

Since GA is strongly bound with boehmite, we can expect antiradical properties in modified NPs. Further, we conducted a series of experiments to assess their cytotoxicity, membrane-protective and antioxidant properties.

3.2. Biological assays

3.2.1. Cytotoxicity (hemolytic activity)

For comparison with hybrid particles solutions of gallic acid were used as reference samples, where its concentration was equal to that in AlOOH-GA-0.5 and AlOOH-GA-2.0 samples and designated as GA-0.5 and GA-2.0.

The study of the hemolytic activity of the solutions (concentration of NPs – 6 mg/ml) showed (Fig. 8) that none of them possesses cytotoxicity, the level of hemolysis in all variants of the experiment did not significantly exceed the spontaneous one. However, aluminum oxyhydroxide and compounds based on it at the indicated concentration (6 mg/ml) caused visible aggregation of cells and their rapid sedimentation to the bottom of the test tubes, which, apparently, is due to the electrostatic interaction of aluminum oxyhydroxide with the surface of the erythrocyte membrane [68].

3.2.2. Membrane-protective activity

It has been established (Table 1) that when the studied solutions are introduced into the suspension of red blood cells in a high concentration (concentration of NPs – 0.6 mg/ml), gallic acid (GA-0.5 and GA-

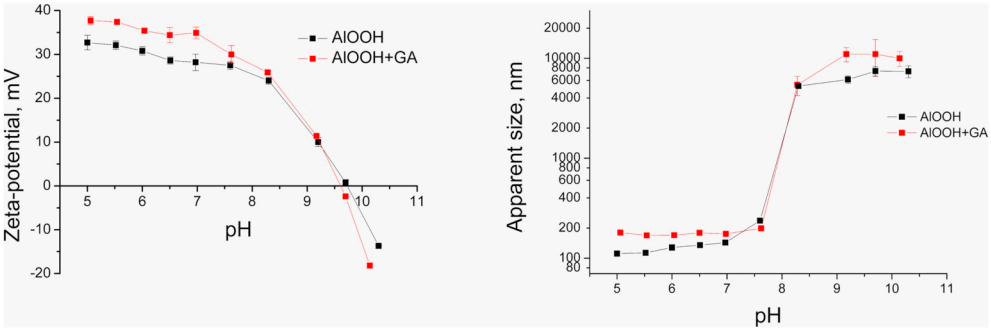

Fig. 5. Dependence of zeta potential (a) and apparent size (b) on pH value of AlOOH and AlOOH-GA sols. (Vertical bars: mean ± SE) (concentration of NPs – 0.6 mg/ml).

2.0), as well as nanoparticles with a high content of gallic acid in the composition (AlOOH-GA-2.0) have a pronounced membrane-protective activity under conditions of acute oxidative stress. Nanoparticles without gallic acid (AlOOH), or with its low content (AlOOH-GA-0.5), lacked a protective effect, but, on the contrary, only increased cell death (Table 1).

By reducing the concentration of test solutions up to five times (concentration of NPs – 0.12 mg/ml) effect changed (Table 2) - the greatest protective activity exhibited nanoparticles containing gallic acid (AlOOH-GA-2.0) but not gallic acid itself (GA-2.0).

With such an experimental design, the negative side effect of aluminum oxyhydroxide disappeared - unmodified nanoparticles (AlOOH) no longer increased cell death under conditions of acute oxidative stress, but, on the contrary, somewhat increased their survival, i.e. possessed weak membrane-protective activity.

Penetrating into the cells, H_2O_2 causes oxidation of oxyhemoglobin, as a result of which the ratios metHb/oxyHb and ferrylHb/oxyHb in the control samples (without studied samples) increases significantly. In samples containing pure aluminum oxyhydroxide and gallic acid modified γ-AlOOH nanoparticles, oxidation of native hemoglobin is less pronounced, and ratios metHb/oxyHb and ferrylHb/oxyHb are significantly lower than in the control (Fig. 9). Solutions of gallic acid lack protective properties against H_2O_2 and give ratios metHb/oxyHb and ferrylHb/oxyHb close to the control.

These protective effects can be associated with the ability of the boehmite surface to form hydrogen bonds with reactive oxygen species and hydrogen peroxide, which was also predicted in theoretical calculations [67].

3.2.3. Non-cellular model (brain homogenates)

Evaluation of the antioxidant activity of compounds using lipids as a substrate for the oxidation of animals showed (Fig. 10) that the solutions of all the studied compounds in various concentrations (concentration of NPs: 0.6 mg/ml; 1.5 mg/ml and 3.0 mg/ml) significantly inhibit the accumulation of secondary products of lipid peroxidation (LPO). The effect is proportional to the concentration of the compounds. Note that in this model system, aluminum oxyhydroxide has a high antioxidant activity, which may be due to its chelating ability. The

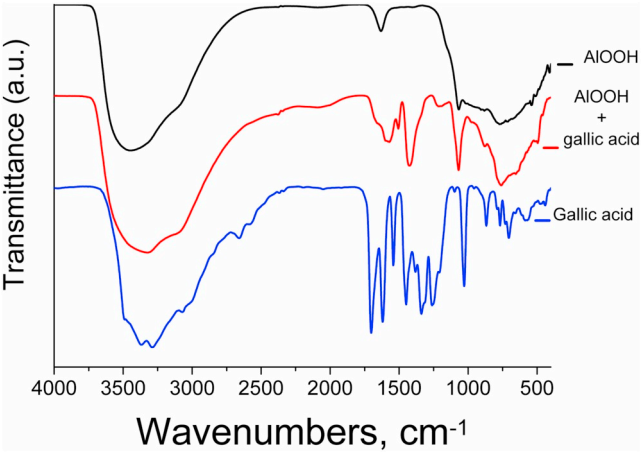

Fig. 7. FTIR spectra of AlOOH, gallic acid and AlOOH-GA-2.0. (Graphs are spaced along the y-axis for clarity).

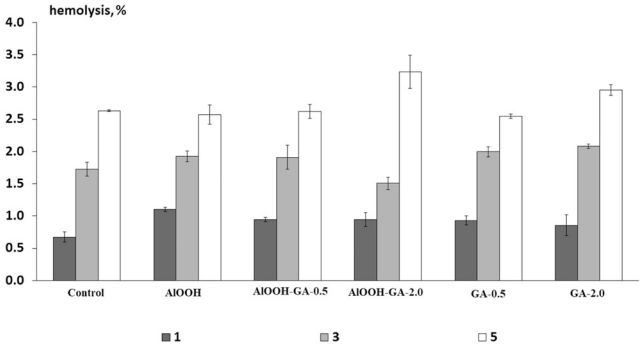

Fig. 8. Hemolytic activity of compounds (cytotoxicity) after 1, 3 and 5 h of incubation (Vertical bars: mean ± SE). (Concentration of NPs – 6.00 mg/ml, concentrations of GA are 0.03 mg/ml and 0.12 mg/ml for GA-0.5 and GA-2.0, respectively).

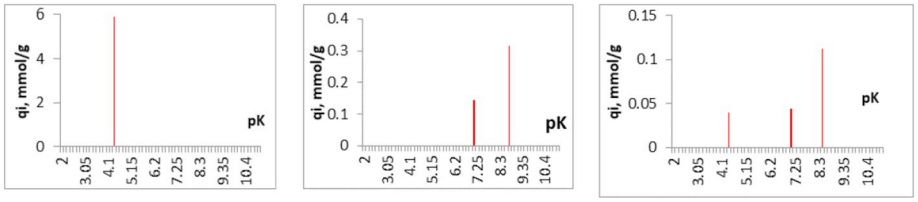

Fig. 6. pK-spectra of gallic acid (a); boehmite (b); hybrid particles boehmite-gallic acid (c). (Concentration of NPs – 6 mg/ml).

Table 1
Comparative evaluation of membrane-protective activity of the derivatives on the model of RBCs oxidative hemolysis (concentration of NPs – 0.600 mg/ml; concentrations of GA are 0.003 mg/ml and 0.012 mg/ml for GA-0.5 and GA-2.0, respectively).

Compound	Membrane-protective activity (hemolysis, %)				
	1 h	2 h	3 h	4 h	5 h
Control	19,0 ± 0,8	43,0 ± 0,6	52,1 ± 0,7	57,2 ± 0,9	62,4 ± 0,9
AlOOH	36,7 ± 1,9	58,8 ± 0,9	59,5 ± 0,8	60,8 ± 0,8	61,5 ± 0,7
AlOOH-GA-0.5	35,3 ± 0,8	53,6 ± 1,0	60,8 ± 0,7	61,2 ± 0,7	61,8 ± 0,6
AlOOH-GA-2.0	20,6 ± 2,4	36,3 ± 1,9	44,6 ± 1,2	47,8 ± 1,0	48,9 ± 0,8
GA-0.5	12,6 ± 0,4	24,7 ± 0,6	36,2 ± 1,8	47,4 ± 1,5	57,8 ± 1,2
GA-2.0	6,4 ± 0,3	13,5 ± 0,6	18,2 ± 1,5	23,0 ± 0,6	27,9 ± 0,5

highest inhibitory activity was observed for nanoparticles with a high content of gallic acid (AlOOH-GA-2.0).

Thus, using the cellular model system (red blood cells of mammals) and non-cellular medium containing animal lipids, a primary assessment of cytotoxicity (hemolytic activity) and antioxidant activity of aluminum oxyhydroxide-based nanoparticles containing gallic acid as an active substance was carried out. The highest antioxidant activity was observed for AlOOH-GA-2.0 nanoparticles with a high content of gallic acid. However, due to the ability of aluminum hydroxide to interact electrostatically with the negatively charged surface of the erythrocyte membrane [68] and cause aggregation and sedimentation of erythrocytes as a result of heterocoagulation, a protective effect in the cell model system can be obtained only with the use of this compound in a relatively low concentration.

4. Conclusions

As a result of the study, boehmite nanoparticles modified with gallic acid were first obtained. Binding between gallic acid and boehmite is strong enough, but can be attributed to various types - covalent and electrostatic. The modified NPs retain a positive charge, IEP, morphology, and crystal structure inherent in the original nanoparticles. Thus, the proposed modification method is soft (ambient temperature and atmospheric pressure), non-destructive and includes only surface interactions. To the best of our knowledge this is the first experimental study confirming boehmite NPs antioxidant activity. Pure boehmite do not induce prooxidant activity, thus it is not toxic for living cells. NPs modified with gallic acid exhibit membrane-protective activity and antioxidant properties. The resulting modified NPs are colloidally stable hydrosols and can be injected into living organisms, but the introduction into the blood in high concentrations can lead to aggregation of red blood cells. In the future, we plan to eliminate this potentially negative effect and expand the range of phytophenolic compounds to modify boehmite nanoparticles.

Declaration of Competing Interest

There are no conflicts to declare.

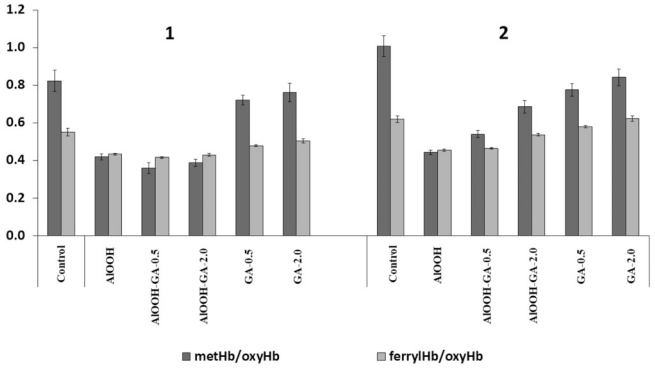

Fig. 9. The effect of the studied solutions on the ratio of native and oxidized forms of hemoglobin in a suspension of red blood cells 5 h after the initiation of H_2O_2 hemolysis. (y-axis - relative units).
(Concentration of NPs: 1–0.6 mg/ml; 2–0.12 mg/ml; concentration of GA in GA-0.5 are 1–0.0030 mg/ml; 2–0.0006 mg/ml and in GA-2.0: 1–0.0120 mg/ml; 2–0.0024 mg/ml).

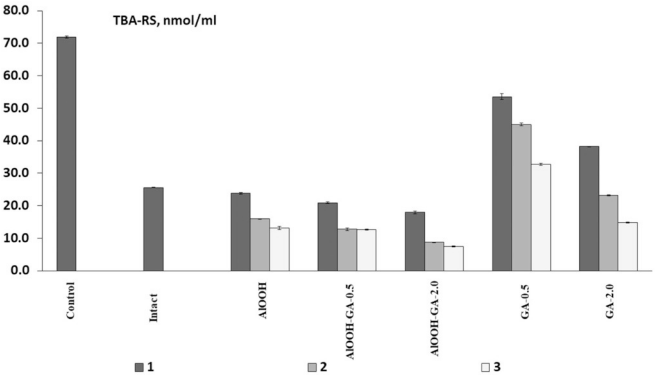

Fig. 10. The effect of the studied solutions on the content of TBARS in the brain homogenate 1 h after the initiation of LPO (concentration of NPs: 1–0.6 mg/ml; 2–1.5 mg/ml; 3–3 mg/ml; concentration of GA in GA-0.5 are 1–0.0030 mg/ml; 2–0.0075 mg/ml; 3–0.0150 mg/ml and in GA-2.0: 1–0.0120 mg/ml; 2–0.0300 mg/ml; 3–0.0600 mg/ml).

Table 2
Comparative evaluation of membrane-protective activity of the derivatives on the model of RBCs oxidative hemolysis (concentration of NPs – 0.1200 mg/ml; concentrations of GA are 0.0006 mg/ml and 0.0240 mg/ml for GA-0.5 and GA-2.0, respectively).

Compound	Membrane-protective activity (hemolysis, %)				
	1 h	2 h	3 h	4 h	5 h
Control	5,5 ± 0,3	37,8 ± 1,5	50,5 ± 2,2	57,3 ± 2,7	62,9 ± 2,8
AlOOH	3,0 ± 0,2	37,6 ± 3,8	45,8 ± 2,3	50,1 ± 0,9	53,4 ± 1,0
AlOOH-GA-0.5	3,7 ± 0,2	30,9 ± 3,3	41,8 ± 1,3	47,2 ± 1,0	51,6 ± 1,1
AlOOH-GA-2.0	3,4 ± 0,2	19,4 ± 1,0	31,6 ± 1,0	41,7 ± 0,7	50,4 ± 2,1
GA-0.5	7,4 ± 0,4	32,5 ± 1,8	45,0 ± 1,6	54,3 ± 1,0	63,7 ± 1,1
GA-2.0	6,1 ± 0,6	26,4 ± 1,4	38,8 ± 1,5	53,7 ± 1,1	67,6 ± 1,4

Acknowledgements

Martakov I. S. is grateful for the financial support by a grant from the Russian Science Foundation (project no. 18-73-00212) for studying processes of preparation hybrid nanoparticles, their properties, mechanism of binding.

Shevchenko O. G. performed studies of cytotoxicity, antioxidant and membrane-protective activities of the NPs on cellular and non-cellular models at the expense of state tasks of the IB of Komi Scientific Center of the Ural Branch of the Russian Academy of Sciences (project № AAAA-A18-118011120004-5).

Researches were carried out with use of equipment of Common Use Centers “Khimiya” (Institute of Chemistry of Komi Science Centre, Ural Branch, Russian Academy of Sciences”) and “Molecular Biology” (Institute of Biology of Komi Science Centre of the Ural Branch of the RAS). The mice of the scientific collection of experimental animals of Institute of Biology of Komi Scientific Centre of the Ural Branch of the RAS were used (http://www.ckp-rf.ru/usu/471933/).

Abbreviations list

NPs	nanoparticles
ROS	reactive oxygen species
GA	gallic acid
TEM	transmission electron microscopy
DLS	dynamic light scattering
FTIR	Fourier-transform infrared
RBCs	red blood cells
PBS	phosphate-buffered saline
TBARS	2-thiobarbituric acid
oxyHb	oxyhemoglobin
metHb	methemoglobin
IEP	isoelectric point
ferrylHb	Ferryl form of hemoglobin
LPO	lipid peroxidation

References

[1] S. Aftab, A. Shah, A. Nadhman, S. Kurbanoglu, S. Aysıl Ozkan, D.D. Dionysiou, S.S. Shukla, T.M. Aminabhavi, Nanomedicine: an effective tool in cancer therapy, Int. J. Pharm. 540 (2018) 132–149, https://doi.org/10.1016/J.IJPHARM.2018.02.007.

[2] M. Manzano, M. Vallet-Regí, Mesoporous silica nanoparticles in nanomedicine applications, J. Mater. Sci. Mater. Med. 29 (2018) 65, , https://doi.org/10.1007/s10856-018-6069-x.

[3] M.A. Mofazzal Jahromi, P. Sahandi Zangabad, S.M. Moosavi Basri, K. Sahandi Zangabad, A. Ghamarypour, A.R. Aref, M. Karimi, M.R. Hamblin, Nanomedicine and advanced technologies for burns: preventing infection and facilitating wound healing, Adv. Drug Deliv. Rev. 123 (2018) 33–64, https://doi.org/10.1016/J.ADDR.2017.08.001.

[4] Y. Li, Y. Wang, G. Huang, J. Gao, Cooperativity principles in self-assembled nanomedicine, Chem. Rev. 118 (2018) 5359–5391, https://doi.org/10.1021/acs.chemrev.8b00195.

[5] H.Y. Yang, Y. Li, D.S. Lee, Multifunctional and stimuli-responsive magnetic nanoparticle-based delivery systems for biomedical applications, Adv. Ther. 1 (2018) 1800011, , https://doi.org/10.1002/adtp.201800011.

[6] R. Dinali, A. Ebrahiminezhad, M. Manley-Harris, Y. Ghasemi, A. Berenjian, Iron oxide nanoparticles in modern microbiology and biotechnology, Crit. Rev. Microbiol. 43 (2017) 493–507, https://doi.org/10.1080/1040841X.2016.1267708.

[7] L.E. Cole, R.D. Ross, J.M.R. Tilley, T. Vargo-Gogola, R.K. Roeder, Gold nanoparticles as contrast agents in x-ray imaging and computed tomography, Nanomedicine 10 (2015) 321–341, https://doi.org/10.2217/nnm.14.171.

[8] J. Estelrich, M.J. Sánchez-Martín, M.A. Busquets, Nanoparticles in magnetic resonance imaging: from simple to dual contrast agents, Int. J. Nanomedicine 10 (2015) 1727–1741, https://doi.org/10.2147/IJN.S76501.

[9] M. Nair, R.D. Jayant, A. Kaushik, V. Sagar, Getting into the brain: potential of nanotechnology in the management of NeuroAIDS, Adv. Drug Deliv. Rev. 103 (2016) 202–217, https://doi.org/10.1016/J.ADDR.2016.02.008.

[10] S. Parveen, R. Misra, S.K. Sahoo, Nanoparticles: a boon to drug delivery, therapeutics, diagnostics and imaging, Nanomedicine Nanotechnology, Biol. Med. 8 (2012) 147–166, https://doi.org/10.1016/J.NANO.2011.05.016.

[11] S.M. Chowdhury, S. Xie, J. Fang, S.K. Lee, B. Sitharaman, Nanoparticle-facilitated membrane depolarization-induced receptor activation: implications on cellular uptake and drug delivery, ACS Biomater. Sci. Eng. 2 (2016) 2153–2161, https://doi.org/10.1021/acsbiomaterials.6b00338.

[12] B. Zhu, Y. Li, Z. Lin, M. Zhao, T. Xu, C. Wang, N. Deng, Silver nanoparticles induce HePG-2 cells apoptosis through ROS-mediated signaling pathways, Nanoscale Res. Lett. 11 (2016) 198, , https://doi.org/10.1186/s11671-016-1419-4.

[13] M. Abdesselem, R. Ramodiharilafy, L. Devys, T. Gacoin, A. Alexandrou, C.I. Bouzigues, Fast quantitative ROS detection based on dual-color single rare-earth nanoparticle imaging reveals signaling pathway kinetics in living cells, Nanoscale 9 (2017) 656–665, https://doi.org/10.1039/C6NR07413H.

[14] V. Sharma, D. Anderson, A. Dhawan, Zinc oxide nanoparticles induce oxidative DNA damage and ROS-triggered mitochondria mediated apoptosis in human liver cells (HepG2), Apoptosis 17 (2012) 852–870, https://doi.org/10.1007/s10495-012-0705-6.

[15] A. Ivanets, M. Roshchina, V. Srivastava, V. Prozorovich, T. Dontsova, S. Nahirniak, V. Pankov, A. Hosseini-Bandegharaei, H. Nguyen Tran, M. Sillanpää, Effect of metal ions adsorption on the efficiency of methylene blue degradation onto MgFe2O4 as Fenton-like catalysts, Colloids Surfaces A Physicochem. Eng. Asp. 571 (2019) 17–26, https://doi.org/10.1016/J.COLSURFA.2019.03.071.

[16] A.I. Ivanets, V. Srivastava, M.Y. Roshchina, M. Sillanpää, V.G. Prozorovich, V.V. Pankov, Magnesium ferrite nanoparticles as a magnetic sorbent for the removal of Mn2+, Co2+, Ni2+ and Cu2+ from aqueous solution, Ceram. Int. 44 (2018) 9097–9104, https://doi.org/10.1016/J.CERAMINT.2018.02.117.

[17] D. Kwatra, A. Venugopal, S. Anant, Nanoparticles in radiation therapy: a summary of various approaches to enhance radiosensitization in cancer, Transl. Cancer Res. 2 (4) (August 2013) Transl. Cancer Res. (Nanotechnology Radiat. Res. (2013) http://tcr.amegroups.com/article/view/1550.

[18] I. Brigger, C. Dubernet, P. Couvreur, Nanoparticles in cancer therapy and diagnosis, Adv. Drug Deliv. Rev. 54 (2002) 631–651, https://doi.org/10.1016/S0169-409X(02)00044-3.

[19] C. Taze, I. Panetas, S. Kalogiannis, K. Feidantsis, G.P. Gallios, G. Kastrinaki, A.G. Konstandopoulos, M. Václavíková, L. Ivanicova, M. Kaloyianni, Toxicity assessment and comparison between two types of iron oxide nanoparticles in Mytilus galloprovincialis, Aquat. Toxicol. 172 (2016) 9–20, https://doi.org/10.1016/J.AQUATOX.2015.12.013.

[20] M. Ghazimoradi, M. Saberi-Karimian, F. Mohammadi, A. Sahebkar, S. Tavallaie, H. Safarian, G.A. Ferns, M. Ghayour-Mobarhan, M. Moohebati, H. Esmaeili, M. Ahmadinejad, The effects of curcumin and curcumin–phospholipid complex on the serum pro-oxidant–antioxidant balance in subjects with metabolic syndrome, Phyther. Res. 31 (2017) 1715–1721, https://doi.org/10.1002/ptr.5899.

[21] J.S. Suk, Q. Xu, N. Kim, J. Hanes, L.M. Ensign, PEGylation as a strategy for improving nanoparticle-based drug and gene delivery, Adv. Drug Deliv. Rev. 99 (2016) 28–51, https://doi.org/10.1016/J.ADDR.2015.09.012.

[22] W.E. Rudzinski, A. Palacios, A. Ahmed, M.A. Lane, T.M. Aminabhavi, Targeted delivery of small interfering RNA to colon cancer cells using chitosan and PEGylated chitosan nanoparticles, Carbohydr. Polym. 147 (2016) 323–332, https://doi.org/10.1016/J.CARBPOL.2016.04.041.

[23] P. Ambigaipalan, Phenolics and polyphenolics in foods, beverages and spices: antioxidant activity and health effects – a review, J. Funct. Foods 18 (2015) 820–897, https://doi.org/10.1016/J.JFF.2015.06.018.

[24] N. Martins, L. Barros, I.C.F.R. Ferreira, In vivo antioxidant activity of phenolic compounds: facts and gaps, Trends Food Sci. Technol. 48 (2016) 1–12, https://doi.org/10.1016/J.TIFS.2015.11.008.

[25] S. Bahrani, M. Ghaedi, A. Daneshfar, Fabrication of size controlled nanocomposite based on zirconium alkoxide for enrichment of gallic acid in biological and herbal tea samples, J. Chromatogr. B 1087–1088 (2018) 14–22, https://doi.org/10.1016/J.JCHROMB.2018.04.021.

[26] Z. Lu, G. Nie, P.S. Belton, H. Tang, B. Zhao, Structure–activity relationship analysis of antioxidant ability and neuroprotective effect of gallic acid derivatives, Neurochem. Int. 48 (2006) 263–274, https://doi.org/10.1016/J.NEUINT.2005.10.010.

[27] S. Maya, T. Prakash, K. Madhu, Assessment of neuroprotective effects of gallic acid against glutamate-induced neurotoxicity in primary rat cortex neuronal culture, Neurochem. Int. 121 (2018) 50–58, https://doi.org/10.1016/J.NEUINT.2018.10.011.

[28] J. Kang, L. Liu, M. Liu, X. Wu, J. Li, Antibacterial activity of gallic acid against Shigella flexneri and its effect on biofilm formation by repressing mdoH gene expression, Food Control 94 (2018) 147–154, https://doi.org/10.1016/J.FOODCONT.2018.07.011.

[29] Â. Luís, F. Silva, S. Sousa, A.P. Duarte, F. Domingues, Antistaphylococcal and biofilm inhibitory activities of gallic, caffeic, and chlorogenic acids, Biofouling 30 (2014) 69–79, https://doi.org/10.1080/08927014.2013.845878.

[30] S.N. Sunil Gowda, S. Rajasowmiya, V. Vadivel, S. Banu Devi, A. Celestin Jerald, S. Marimuthu, N. Devipriya, Gallic acid-coated sliver nanoparticle alters the expression of radiation-induced epithelial-mesenchymal transition in non-small lung cancer cells, Toxicol. Vitr. 52 (2018) 170–177, https://doi.org/10.1016/J.TIV.2018.06.015.

[31] D. Li, Z. Liu, Y. Yuan, Y. Liu, F. Niu, Green synthesis of gallic acid-coated silver nanoparticles with high antimicrobial activity and low cytotoxicity to normal cells, Process Biochem. 50 (2015) 357–366, https://doi.org/10.1016/J.PROCBIO.2015.01.002.

[32] I.Y. Tóth, M. Szekeres, R. Turcu, S. Sáringer, E. Illés, D. Nesztor, E. Tombácz, Mechanism of in situ surface polymerization of gallic acid in an environmental-inspired preparation of carboxylated core–shell magnetite nanoparticles, Langmuir 30 (2014) 15451–15461, https://doi.org/10.1021/la5038102.

[33] S. Iraji, F. Ganji, L. Rashidi, Surface modified mesoporous silica nanoparticles as sustained-release gallic acid nano-carriers, J. Drug Deliv. Sci. Technol. 47 (2018) 468–476, https://doi.org/10.1016/J.JDDST.2018.08.008.

[34] M. Suwalsky, F. Villena, B. Norris, Y.F. Cuevas, C.P. Sotomayor, P. Zatta, Effects of lead on the human erythrocyte membrane and molecular models, J. Inorg. Biochem. 97 (2003) 308–313, https://doi.org/10.1016/S0162-0134(03)00292-7.
[35] M. Suwalsky, P. Fierro, F. Villena, C.P. Sotomayor, Effects of lithium on the human erythrocyte membrane and molecular models, Biophys. Chem. 129 (2007) 36–42, https://doi.org/10.1016/J.BPC.2007.05.003.
[36] A. Kumar, M. Ali, B.N. Pandey, P.A. Hassan, K.P. Mishra, Role of membrane sialic acid and glycophorin protein in thorium induced aggregation and hemolysis of human erythrocytes, Biochimie 92 (2010) 869–879, https://doi.org/10.1016/J.BIOCHI.2010.03.008.
[37] I. Baranowska-Bosiacka, V. Dziedziejko, K. Safranow, I. Gutowska, M. Marchlewicz, B. Dołęgowska, M.E. Rać, B. Wiszniewska, D. Chlubek, Inhibition of erythrocyte phosphoribosyltransferases (APRT and HPRT) by Pb2+: a potential mechanism of lead toxicity, Toxicology 259 (2009) 77–83, https://doi.org/10.1016/J.TOX.2009.02.005.
[38] V.P.P. Schiar, D.B. dos Santos, M.W. Paixão, C.W. Nogueira, J.B.T. Rocha, G. Zeni, Human erythrocyte hemolysis induced by selenium and tellurium compounds increased by GSH or glucose: a possible involvement of reactive oxygen species, Chem. Biol. Interact. 177 (2009) 28–33, https://doi.org/10.1016/J.CBI.2008.10.007.
[39] E. Niki, E. Komuro, M. Takahashi, S. Urano, E. Ito, K. Terao, Oxidative hemolysis of erythrocytes and its inhibition by free radical scavengers, J. Biol. Chem. 263 (1988) 19809–19814.
[40] F.N. Ko, G. Hsiao, Y.H. Kuo, Protection of oxidative hemolysis by demethyldiisoeugenol in normal and β-thalassemic red blood cells, Free Radic. Biol. Med. 22 (1997) 215–222, https://doi.org/10.1016/S0891-5849(96)00295-X.
[41] J. Takebayashi, J. Chen, A. Tai, D. Armstrong (Ed.), A Method for Evaluation of Antioxidant Activity Based on Inhibition of Free Radical-Induced Erythrocyte Hemolysis BT - Advanced Protocols in Oxidative Stress II, Humana Press, Totowa, NJ, 2010, pp. 287–296, , https://doi.org/10.1007/978-1-60761-411-1_20.
[42] C.I. Acker, R. Brandão, A.R. Rosário, C.W. Nogueira, Antioxidant effect of alkynylselenoalcohol compounds on liver and brain of rats in vitro, Environ. Toxicol. Pharmacol. 28 (2009) 280–287, https://doi.org/10.1016/J.ETAP.2009.05.002.
[43] N.A.V. Bellé, G.D. Dalmolin, G. Fonini, M.A. Rubin, J.B.T. Rocha, Polyamines reduces lipid peroxidation induced by different pro-oxidant agents, Brain Res. 1008 (2004) 245–251, https://doi.org/10.1016/J.BRAINRES.2004.02.036.
[44] P. Chaudhary, Antioxidant activity of fractionated extracts of rhizomes of high-altitude Podophyllum hexandrum: role in radiation protection, Mol. Cell. Biochem. 273 (1–2) (2005) 193–208.
[45] P. Costa, S. Gonçalves, P.B. Andrade, P. Valentão, A. Romano, Inhibitory effect of Lavandula viridis on Fe2+-induced lipid peroxidation, antioxidant and anti-cholinesterase properties, Food Chem. 126 (2011) 1779–1786, https://doi.org/10.1016/J.FOODCHEM.2010.12.085.
[46] J.-S. Kim, Preliminary evaluation for comparative antioxidant activity in the water and ethanol extracts of dried citrus fruit (< i > Citrus unshiu < /i >) peel using chemical and biochemical < i > in vitro < /i > assays, Food Nutr. Sci. 04 (2013) 177–188, https://doi.org/10.4236/fns.2013.42025.
[47] S.N. Lim, P.C.K. Cheung, V.E.C. Ooi, P.O. Ang, Evaluation of Antioxidative activity of extracts from a brown seaweed, Sargassum siliquastrum, J. Agric. Food Chem. 50 (2002) 3862–3866, https://doi.org/10.1021/jf020096b.
[48] G. Oboh, R.L. Puntel, J.B.T. Rocha, Hot pepper (Capsicum annuum, Tepin and Capsicum Chinese, Habanero) prevents Fe2+-induced lipid peroxidation in brain – in vitro, Food Chem. 102 (2007) 178–185, https://doi.org/10.1016/J.FOODCHEM.2006.05.048.
[49] S.T. Stefanello, A.S. Prestes, T. Ogunmoyole, S.M. Salman, R.S. Schwab, C.R. Brender, L. Dornelles, J.B.T. Rocha, F.A.A. Soares, Evaluation of in vitro antioxidant effect of new mono and diselenides, Toxicol. Vitr. 27 (2013) 1433–1439, https://doi.org/10.1016/J.TIV.2013.03.001.
[50] A. Rutenberg, V.V. Vinogradov, D. Avnir, Synthesis and enhanced thermal stability of albumins@alumina: towards injectable sol–gel materials, Chem. Commun. 49 (2013) 5636–5638, https://doi.org/10.1039/C3CC41696H.
[51] B. Sun, Z. Ji, Y.-P. Liao, M. Wang, X. Wang, J. Dong, C. Hyun Chang, R. Li, H. Zhang, A.E. Nel, T. Xia, Engineering an effective immune adjuvant by designed control of shape and crystallinity of aluminum oxyhydroxide nanoparticles, ACS Nano 7 (2013) 10834–10849, https://doi.org/10.1021/nn404211j.
[52] C. Exley, The pro-oxidant activity of aluminum, Free Radic. Biol. Med. 36 (2004) 380–387, https://doi.org/10.1016/J.FREERADBIOMED.2003.11.017.
[53] B.E. Yoldas, Hydrolysis of aluminum alkoxides and bayerite conversion, J. Appl. Chem. Biotechnol. 23 (1973) 803–809.
[54] M.A. Ryazanov, B.N. Dudkin, Acid-base properties of the surface of the α-Al2O3 suspension, Russ. J. Phys. Chem. A 83 (2009) 2318–2321, https://doi.org/10.1134/S0036024409130238.
[55] V.L. Singleton, R. Orthofer, R.M. Lamuela-Raventós, [14] Analysis of total phenols and other oxidation substrates and antioxidants by means of folin-ciocalteu reagent, Methods Enzymol. 299 (1999) 152–178, https://doi.org/10.1016/S0076-6879(99)99017-1.
[56] T. Asakawa, S. Matsushita, Coloring conditions of thiobarbituric acid test for detecting lipid hydroperoxides, Lipids 15 (1980) 137–140, https://doi.org/10.1007/BF02540959.
[57] J.J.M. van den Berg, J.A.F. Op den Kamp, B.H. Lubin, B. Roelofsen, F.A. Kuypers, Kinetics and site specificity of hydroperoxide-induced oxidative damage in red blood cells, Free Radic. Biol. Med. 12 (1992) 487–498, https://doi.org/10.1016/0891-5849(92)90102-M.
[58] A. Takagaki, J.C. Jung, S. Hayashi, Solid Lewis acidity of boehmite γ-AlO(OH) and its catalytic activity for transformation of sugars in water, RSC Adv. 4 (2014) 43785–43791, https://doi.org/10.1039/C4RA08061K.
[59] J.A. Kellum, Determinants of blood pH in health and disease, Crit. Care 4 (2000) 6, https://doi.org/10.1186/cc644.
[60] N.K. Iversen, H. Malte, E. Baatrup, T. Wang, The normal acid–base status of mice, Respir. Physiol. Neurobiol. 180 (2012) 252–257, https://doi.org/10.1016/J.RESP.2011.11.015.
[61] K. Bourikas, C. Kordulis, A. Lycourghiotis, The mechanism of the protonation of metal (hydr)oxides in aqueous solutions studied for various interfacial/surface ionization models and physicochemical parameters: a critical review and a novel approach, Adv. Colloid Interf. Sci. 121 (2006) 111–130, https://doi.org/10.1016/J.CIS.2006.06.002.
[62] A.E. Fazary, Y.-H. Ju, Nonaqueous solution studies on the protonation equilibria of some phenolic acids, J. Solut. Chem. 37 (2008) 1305–1319, https://doi.org/10.1007/s10953-008-9305-z.
[63] J.C. Bolger, K.L. Mittal (Ed.), Acid Base Interactions between Oxide Surfaces and Polar Organic Compounds BT - Adhesion Aspects of Polymeric Coatings, Springer US, Boston, MA, 1983, pp. 3–18, , https://doi.org/10.1007/978-1-4613-3658-7_1.
[64] C.J. Serna, J.L. White, S.L. Hem, Hydrolysis of aluminum-tri-(sec-butoxide) in ionic and nonionic media, Clay Clay Miner. 25 (1977) 384–391, https://doi.org/10.1346/CCMN.1977.0250603.
[65] X. GUAN, G. CHEN, C. SHANG, ATR-FTIR and XPS study on the structure of complexes formed upon the adsorption of simple organic acids on aluminum hydroxide, J. Environ. Sci. 19 (2007) 438–443, https://doi.org/10.1016/S1001-0742(07)60073-4.
[66] X.-H. Guan, C. Shang, G.-H. Chen, ATR-FTIR investigation of the role of phenolic groups in the interaction of some NOM model compounds with aluminum hydroxide, Chemosphere 65 (2006) 2074–2081, https://doi.org/10.1016/j.chemosphere.2006.06.048.
[67] T. Ribeiro, A. Motta, P. Marcus, M.-P. Gaigeot, X. Lopez, D. Costa, Formation of the OOH radical at steps of the boehmite surface and its inhibition by gallic acid: a theoretical study including DFT-based dynamics, J. Inorg. Biochem. 128 (2013) 164–173, https://doi.org/10.1016/J.JINORGBIO.2013.07.024.
[68] F. Tokumasu, G.R. Ostera, C. Amaratunga, R.M. Fairhurst, Modifications in erythrocyte membrane zeta potential by plasmodium falciparum infection, Exp. Parasitol. 131 (2012) 245–251, https://doi.org/10.1016/J.EXPPARA.2012.03.005.